LA-UR- 93-194

Title: APPLICATION OF AN ADVANCED ATMOSPHERIC MESOSCALE MODEL TO DISPERSION IN THE ROCKY FLATS, COLORADO VICINITY

LA-UR--93-194

DE93 007383

Author(s): Gregory S. Poulos, EES-5
James E. Bossert, EES-5

Submitted to: International Specialty Conference, January 26-28, 1993

DISTRIBUTION OF THIS DOCUMENT IS UNLIMITED

DISCLAIMER

MASTER

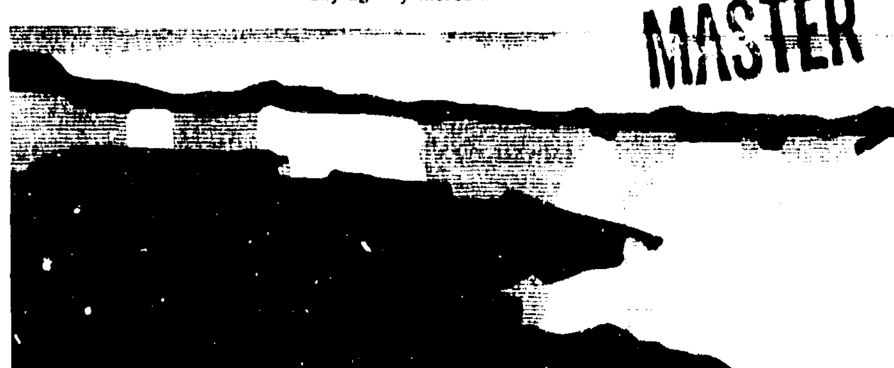

Los Alamos
NATIONAL LABORATORY

Form No. 836 R5
ST 2629 10/91

Application of an Advanced Atmospheric Mesoscale Model to Dispersion in the Rocky Flats, Colorado Vicinity

Gregory S. Poulos and James E. Bossert
Earth and Environmental Sciences Division
Los Alamos National Laboratory, Los Alamos, New Mexico 87545

ABSTRACT

The Atmospheric Studies in Complex Terrain (ASCOT) program sponsored a field experiment in the winter of 1991 near Rocky Flats, Colorado. Both meteorological and tracer dispersion measurements were taken. These two data sets provided an opportunity to investigate the influence of terrain-generated, radiatively-driven flows on the dispersion of the tracer. We use the Regional Atmospheric Modeling System (RAMS), originally developed at Colorado State University, to simulate meteorological conditions and tracer dispersion on the case night of 4-5 February 1991. The simulations described herein reveal considerable information about the extent to which the Rocky Mountains influence the flow along the Front Range , the importance of diffusion when simulating drainage flows and the computing needs of simulations in complex terrain regions.

1. Introduction

In January/February, 1991 an intensive set of measurements was taken around Rocky Flats near Denver, CO under the auspices of the Department of Energy's Atmospheric Studies in Complex Terrain (ASCOT) program. This region of the country, known as the Front Range, is characterized by a transition from the gently sloping terrain of the Great Plains to the highly varied terrain of the Rocky Mountains. The mountains are oriented north south and rise from 1800 m above mean sea level (MSL) to 3600 m MSL at the Continental Divide (see Figure 1). Numerous east west oriented valleys begin in the mountains and end at the plains interface. Flows from two of these canyons, specifically Eldorado and Coal Creek Canyons, were suspected of influencing the Rocky Flats region. This highly complex terrain of various scales makes the Front Range a challenging region in which to study windflows. One of the windflows generated by this severe terrain that is significant to the human population along the Front Range are the drainage winds found during stagnant, wintertime conditions. Not only do drainage flows occur during weather conditions conducive to pollutant accumulation, but they are primarily a surface flow, influencing where near-surface pollutants are transported. Since drainage conditions occur frequently along the Front Range, ASCOT is investigating how these flows interact with larger-scale mountain and synoptic winds. This, in turn, will improve our ability to model the dispersion of pollutants from Front Range cities and industrial sites.

The ASCOT 1991 data included surface and upper air measurements on approximately a 50 km^2 scale. Simultaneously, an SF_6 tracer release study was being conducted around Rocky Flats, a nuclear materials production facility. This combination of meteorological and tracer concentration data provided a unique data set for comparisons of mesoscale and dispersion modeling results with observations and for evaluating our capability to predict pollutant transport.

Our approach in utilizing this data set is to use the Regional Atmospheric Modeling System (RAMS) mesoscale model to simulate atmospheric conditions and the Lagrangian Particle Dispersion Model (LPDM), a component of the RAMS system, to model the dispersion of the SF_6. We have concentrated on the 4-5 February 1991 overnight period as our case study, although some discussion of other case nights will be made. This night was characterized by strong drainage flows from the Rocky Mountains to the west of Rocky Flats, southerly winds in a layer about 1 km in depth above the drainage flows (these southerlies occasionally would reach the surface), and northwesterly winds above that layer extending to the tropopause.

The authors would like to note that this paper represents an extension from work published previously by the authors, specifically Poulos and Bossert (1992a) and Poulos and Bossert (1992b). In the course of our research progress, some improvements have been made to the particle model code and more appropriate initial model conditions have been implemented. These improvements alter the conclusions of those studies somewhat. Most of the general conclusions of those papers are unaffected by the modifications and are reiterated here.

2. The Mesoscale Model

RAMS is a three dimensional, atmospheric primitive equation, mesoscale model that uses terrain following coordinates as described in Tremback et al. (1986), Cotton et al. (1988) and Tremback and Walko (1991). It was conceived by the unification of a non hydrostatic cloud model and two hydrostatic mesoscale models at Colorado State University in the early 1980's. Surface energy balance is maintained via formulations of radiative fluxes (Chen and Cotton, 1983a,b), latent and sensible heat fluxes, and sub surface heat conduction from an 11 level soil temperature model (Tremback and Kessler, 1985). RAMS uses finite difference grid techniques where the grid spacing and the number of grid spaces is specified by the user to create the model domain. Within this domain, a feature of RAMS allows the user to specify additional grids of smaller grid spacing (called 'nests'), thereby focusing on the region of interest with higher resolution. Widely varying atmospheric phenomena have been successfully studied using this flexible code.

ranging from turbulent eddies to synoptic-scale weather systems and from mid-latitude tornadoes to subtropical thunderstorms.

In this study we report on simulations completed using RAMS over the Rocky Flats region for the ASCOT 1991 measurement program. Results from the model are compared to observations of wind and temperature structure. We attempt to capture the drainage flow characteristics as well as the upper air wind development on very small scales because drainage flows are often shallow, local features and the terrain in which it is generated is highly-variable. We use two basic approaches to simulating our case days. The first is to use zero initial winds with the temperature and moisture profiles of the case day. This approach allows us to simulate the thermally-driven drainage flows that develop without the complicating influence of ambient flow. In the second approach we include the observed ambient windspeed and direction. In this case, drainage flows that develop overnight are subject to additional interactions with upper level flow. Because we are using the RAMS code in the fully prognostic mode this second approach provides a forecast of meteorological conditions and dispersion.

Our basic grid configuration is depicted in Figure 1. The outermost grid, Grid 1, has 6 km grid spacing. The first nested grid, Grid 2, and the second nested grid, Grid 3, have 1.5 km and 500 m grid spacing respectively. Grids 1, 2 and 3 have 28x30 (168x180 km), 30x26 (45x39 km) and 32x38 (16x19 km) gridpoints in the east-west and north-south directions (Figure 1) horizontally, respectively. The finest grid (Grid 3) is centered over the canyons to the west of Rocky Flats to accurately resolve the mountain-valley-plains transition. Of 30 gridpoints vertically, there are five (5) 20 meter levels in the first 100 meters of model atmosphere to represent the vertical structure of low-level drainage flows with high resolution. Above 100 m the grid-spacing gradually stretches to 1000 m and then remains constant until reaching the model top at 15.8 km.

3. The Dispersion Model

The meteorological variables output from RAMS are used as input to the LPDM which has been described by Pielke (1984) and McNider et al. (1988). In the LPDM, a point source can be placed at any location within the RAMS model domain with any specified release rate. Particles released into the model domain are then advected from windfields prognosed by RAMS. A parameterized subgrid scale turbulent velocity component is also applied to each particle as it is advected. In this study, a point source is initiated at 2000 LST at Rocky Flats to match the release of the tracer exactly during the experimental period. One particle is released every 10 seconds at 2 m above ground level (AGL) until 0700 LST the following morning. Both particle locations and concentrations from the LPDM were analyzed at hourly intervals for each of the RAMS simulations. A diagnostic particle simulation of point sources within Eldorado and Coal Creek Canyons similar to the above mentioned Rocky Flats release in time and rate was also completed.

In working with the LPDM code, the authors noted that under the very stable nocturnal conditions simulated, both horizontal and vertical dispersion were very limited compared to observations. We first investigated the use of the second order closure work of Blackadar(1979) in calculating σ''_w (see McNider et al., 1988). Blackadar's (1979) formulation appears as

$$\sigma''_w = 1.2l^2[(R_c - Ri)/R_c]^{0.58}\left|\frac{dV}{dz}\right|, \tag{1}$$

where σ''_w is the standard deviation of the subgrid scale vertical velocity, l is the mixing length, dV/dz is the wind shear, Ri is the gradient Richardson number and R_c is the critical Richardson number. This equation is only invoked during stable conditions and is limited to values greater than or equal to zero. One can see, however, that when Ri exceeds R_c the result will be negative. In this instance, however, model code sets σ''_w to zero, implying laminar conditions. This coding, though following Blackadar's theory, eliminates the vertical turbulent component quite frequently in stable atmospheric conditions, creating unrealistically small vertical dispersion. In fact, in our simulation of drainage flows, the Richardson number most always exceeded R_c which is typically 0.25. Given observations of considerable vertical transport of the Rocky Flats plume during the experiment, we suspected this limitation imposed by the Blackadar formulation to be too severe for reality. Further investigation of this problem led us to the *hysteresis* effect for turbulence in the atmosphere when its' existence is based upon Richardson number (Stull,1991):

> "Theoretical and laboratory research suggest that laminar flow becomes unstable to Kelvin-Helmholtz wave formation when Ri is smaller than the *critical Richardson number*, R_c. Another value R_T indicates the termination of turbulence. The dynamic stability criteria can be stated as follows:
>
> Laminar flow becomes turbulent when Ri $<$ R_c.
>
> Turbulent flow becomes laminar when Ri $>$ R_T.
>
> Although there is still some debate on the correct value...R_T = 1.0 works fairly well."

Since our simulations are based on a transition from the turbulent conditions of the daytime to the progressively more stable conditions overnight, R_T seemed a more appropriate candidate in (1) than R_c. Our modification to (1) then, is:

$$\sigma''_w = 1.2l^2[(R_T - Ri)/R_T]^{0.58}\left|\frac{dV}{dz}\right|, \tag{2}$$

where R_T = 1.0 and indicates the termination of turbulence (flow becomes laminar). Additionally, a lower limit on σ''_w of 0.05 was used based on measurements (Haugen et al.,1971, Businger et al., 1971) and calculations (Andre et al.,1978) of u_* (friction velocity) and σ''_w/u_* (Caughey et al,1979) in stable conditions. Based on these measurements both u_*, and therefore σ''_w, appear to minimize close to 0.05. We therefore chose to limit both u_* and σ''_w to 0.05 in the LPDM formulation.

We next investigated the calculation of the standard deviations of the horizontal subgrid scale velocity components σ_u'' and σ_v'' in the LPDM. From McNider et al. (1988) and Panofsky et al. (1977),

$$\sigma_u'' = \sigma_v'' = 2.3u_*. \tag{3}$$

Since our investigation of σ_w'' found a minimum of 0.05 for u_*, we also used this as a lower bound in the LPDM calculation of σ_u'' and σ_v''. The use of these formulations improved the vertical and lateral dispersion within the LPDM, providing a closer match to observations.

4. Zero Initial Wind Simulations

In the zero initial wind simulations the model is integrated for 19 hours (1500 to 1000 LST) from initial horizontally homogeneous conditions, based upon observed temperature and moisture soundings. By using the zero initial wind configuration, only radiatively-driven (drainage) flows were generated. Simulation 1 uses topography derived from a 30-second terrain data set, smoothed with a silhouette averaging scheme that preserves realistic topography heights. Simulation 2 eliminates the gentle slope of the Great Plains by replacing the slope with a 2000 m MSL plain with the purpose of investigating the Rocky Mountain drainage influence alone. Simulation 3 eliminates the Rocky Mountains, but retains realistic Great Plains topography to obviate the Great Plains drainage contribution. The model domain in each simulation, except for Simulation 3 which only requires one grid of 1.5 km grid spacing due to its' simple topography, was described in Section 2.

a. Simulation 1: Realistic Topography

After initial start-up at 1500 LST, approximately two hours of simulated radiative weak wintertime heating occur before sundown, producing a general upslope flow over the region (not shown). This flow appears to be strongly terrain influenced with the highest magnitudes in steeper topography regions. Also, small scale terrain variations to the east of Rocky Flats create a convergence area on the bench upon which Rocky Flats sits. The simulated transition from up- to downslope drainage flow occurs at approximately 1730 LST (Figure 2). Observations showed this transition to occur closer to 1630 LST. The transition to drainage flow (complete reversal) occurs over approximately 45 minutes.

By 2000 LST a consistent, terrain induced, drainage flow has established itself throughout the domain which continues through the morning hours (Figure 3, 0400 LST). The magnitude of the simulated drainage flows are 3.0 to 7.0 ms^{-1} consistent with observations (Figure 4) at this time, and they remain approximately so throughout the drainage period. The simulated wind vectors all have a dominant westerly component, matching favorably to the observed winds. Canyons with larger drainage areas (i.e. Ralston Creek and Eldorado Canyons) contain stronger drainage flows than smaller canyons (i.e. Coal Creek Canyon). These flows appear to 'spill' out onto the plains.

Figure 5 shows the wind vectors on Grid 3 at 50 m AGL at 0400 LST. Note how an increase in resolution affects terrain depiction (compare Figure 5 to Figure 3). As in Figure 3 the winds from the canyons influence flows on the plains. This influence affects the general downslope on the plains to an extent relative to the canyon size. Eldorado Canyon's drainage appears to extend its' influence as much as 15 km onto the plains, whereas Coal Creek's influence ends at less than 2 km. At the surface the canyon flows do not affect the plains flows as extensively as at the 50 m AGL level. Surface friction appears to reduce the effect of surface level canyon drainage. Upper level model profiles of wind also indicate a reduced influence of the canyon drainage with height.

Vertical cross sections parallel to the canyon axes (Figure 6, Coal Creek Canyon, Figure 7, Eldorado Canyon) and parallel to the mountains (Figure 8) show detailed vertical structure. The core of radiatively driven drainage out of Coal Creek Canyon is approximately 100-200 m deep once it has developed (Figure 6a). Note in Figure 6b how the potential temperature structure corresponds to the downslope flow structure. The highest drainage windspeeds are found in the lowest 50 m AGL, the most stable portion of the vertical profile. The wind structure varies considerably from 2300 to 0700 LST reaching a maximum speed of 4.0 ms^{-1} by 0100 LST. This maximum is less than the observed maximum of 7.0 ms^{-1} measured by lidar at the mouth of Coal Creek (Coulter and Martin, 1991).

The vertical structure of Eldorado Canyon drainage is deeper (200-300 m, see Figure 7) and of greater breadth (Figure 8) than Coal Creek Canyon. Apparently the greater drainage basin area of Eldorado Canyon compared to Coal Creek Canyon also contributes to a greater maximum simulated drainage velocity of 8.0 ms^{-1}. In Figure 7b we can see the deeper and more consistent stable layer in Eldorado Canyon. At the location of Gross Reservoir (approximately -21.0 to -22 km), where the terrain aspect changes relative to the canyon drainage direction, a considerable cold pool develops. This cold pool regularly builds up and 'spills' over this terrain feature overnight.

Figures 8a and b, display north-south cross sections of drainage core structure at 2000 and 0200 LST, respectively, just beyond the canyon mouths. Figure 8 reveals the development and strengthening of a drainage core in Eldorado Canyon over time. The Ralston Creek Canyon drainage also shows similar characteristics. Coal Creek Canyon, however, shows considerably weaker drainage influence and structure at this location east of the canyon mouths. Elevated cores of flow develop in each of the three canyons to varying degrees. Although its' influence was not of specific interest to the dispersion from Rocky Flats as were Eldorado and Coal Creek Canyons, Ralston Creek Canyon appears to develop significant elevation to its drainage core. By 0200 LST Eldorado, Coal Creek and Ralston Creek Canyons have elevated cores at approximately 30 m, 20 m and 90 m, respectively. The Coal Creek Canyon minisodar indicated that the drainage core varied from 40 m to 60 m. In each canyon, the maximum drainage speed alternates from an elevated to surface location at various times over the simulated period. Apparently, upstream undulations in canyon shape create an environment where drainage flows can develop complex vertical structure. Despite its shortcomings, this sequence of simulated overnight drainage development reveals that observed elevated drainage cores can be depicted when modeled with sufficient resolution.

Interestingly, the simulated drainage flows appear to excite transient vertically propagating gravity waves in this zero-ambient flow (initially) environment. We suspect that gravity waves occur in most complex terrain drainage conditions but their effect is seldom measured due to damping layers aloft or the dominance of ambient flows. In an excellent review of internal gravity waves and turbulence Moran (1992) explains that stratified flows in complex terrain are a frequent initiation mechanism for gravity waves; on a smaller scale, then, stably stratified drainage flows could excite gravity waves when flowing over local terrain features. Davis and Peltier (1976) suggest local shear in stable flow conditions could also excite gravity waves. It appears that more investigation into drainage flow-induced gravity wave mechanisms is certainly warranted.

These model results and comparisons to observations suggest strongly that for the overnight period of 4-5 February 1991 low-level flow within 2 km of the mountains was, in part, controlled by katabatic winds created by the general slope of the Rocky Mountains, **but** the small-scale variations in drainage induced by the canyons **did not** affect the plains drainage significantly. That is, the details of drainage flow direction and speed from small-scale terrain features (such as canyons) are mostly undetectable at Rocky Flats which is approximately 6 km from the mountain-plains interface. In the case of larger canyons (i.e. Eldorado and Ralston Creek Canyons) drainage influence can, at times, reach as far as 15 km onto the plains. If a drainage from Eldorado Canyon were to be diverted somewhat towards the south, it could impact Rocky Flats based on our simulations. In general, however, the flows at Rocky Flats appear to be locally driven on this case night, with occasional influence from Eldorado Canyon. The latter portion of this statement agrees with the observations of Banta (1992). We investigate these conclusions further by simulating the dispersion of the Rocky Flats SF_6 tracer release for 4-5 Feb 1991.

b. Simulation 1: Rocky Flats Dispersion

The LPDM was integrated for the entire SF_6 release period, 2000-0700 LST. The actual tracer release rate of 12.16 kg hr^{-1} was matched exactly in the model. Figure 9 provides an example of how the tracer release observations (dotted line, from Shearer, 1992) compared to the simulated dispersion (solid contours) of SF_6 at two different times. The inner and outer arcs on Figure 9 are composed of sampling sites at 8 km and 16 km radius from the release point, respectively. In the 2300 0000 average (Figure 9a) the plume dispersion comparison is close with respect to concentration, but the direction of transport is rotated approximately 15 degrees. The two most obvious other inaccuracies are that 1) the actual plume at this time has moved farther than the model plume, and 2) the model plume does not bend to the north.

The 0200 0300 LST concentration average (Figure 9b) observed plume shows a surface structure that spreads gradually eastward and northeastward with a southerly lobe. The primary difference in the actual plume compared to the model simulation is the extent of this southerly lobe. There is some indication of a lobe forming to the south of the centerline in the model plume, but it is far less extensive than in the observations. For the most part simulated plume transport follows drainage routes towar' the South Platte River Valley to the northeast of Rocky Flats as did the observed plume. We suspect that the reason our model plume differs from the observed plume is the zero ambient flow initial condition used in the model, which eliminates the potential influence of non-radiatively driven flows on plume structure and transport. That the modeled plume is quite comparable in shape and length to observations throughout the simulation, despite this being a purely radiatively driven simulation, is strong evidence that larger-scale flows were not the primary mechanism of plume transport for this case study. This further implies that in the Rocky Flats vicinity multi-scale meteorological interactions were not strongly occurring on this night.

c. Simulation 1: Canyon Dispersion

To shed further light on the influence of drainage flows on dispersion in the Rocky Flats area a LPDM simulation was completed with a point source in Eldorado and Coal Creek Canyons. Similar to the tracer simulation particles were released every 40 seconds and for the same 11 hour period (2000-0700 LST, 4-5 February 1991). Figure 10 shows the x-y particle positions for this case at 0300 LST. While it is difficult for the reader to understand the time sequence of transport from this Figure, one can see the two distinct plumes rather well. The Eldorado Canyon plume begins with little lateral dispersion deep within the canyon drainage. In time there is a tendency for particles to be transported to the west-southwest toward Rocky Flats in a coherent fashion. This could be a clue that Eldorado Canyon's drainage is penetrating the plains drainage at least 4 km. Once in the vicinity of Rocky Flats, particles from Eldorado Canyon move off to the northeast caught in the general South Platte River drainage. In contrast, the particles released from Coal Creek Canyon take a distinct transport route toward Denver. In this sense then, the flows from each canyon tend to take routes around the Rocky Flats bench (topographical feature). Given this tendency, it would appear from this simulation that particles released from Rocky Flats could follow either the South Platte River to the north and east or travel toward Denver to the south and east depending on slight influences to the north or south from regional or upper level winds.

d. Simulation 2: Realistic mountains, flat plains

Observations overnight on 4-5 Feb 1991 with a horizontal scanning lidar (Banta, 1992) indicated that the Eldorado Canyon drainage would often shift to the north or south from a generally easterly direction, occasionally passing over the Rocky Flats plant. This could have either been due to periodic influence from ambient winds aloft, a regular regional plains drainage interaction or some form of momentum pulsation from tributary drainage or other terrain influence in Eldorado Canyon. Obviously, only the second and third mechanisms could be simulated in this zero wind initialization investigation.

Figure 11 shows the u component of the wind on Grid 2 from the flat plains simulation. By this time, 0400 LST, drainage flow out of every major canyon encompassed by Grid 2 is obvious. Note however that comparatively smaller Coal Creek Canyon does not appear to show significant drainage. Of course, we know that on Grid 3 (see Figure 6) which had

500 m grid-spacing, Coal Creek did drain significantly. This illustrates the importance of resolution when simulating complex terrain regions, and the effect of averaging 500 m grid spacing (Grid 3) information up to a 1500 m grid spacing (Grid 2) plot. Still, insufficient resolution may explain why the simulated Coal Creek drainage is less than the observations (Coulter and Martin, 1991) of drainage winds up to 7.0 ms^{-1} in Coal Creek Canyon.

Figure 11 does show significant influence from Eldorado Canyon onto the plains however. From the canyon mouth, (approximately X point 17.5 km) flow from Eldorado Canyon extends about 18 km to the east. The extent is less near the surface than at 50 m and also lessens above this level. A time sequence of jet behavior reveals only small perturbations to the north and south from the easterly direction. Since our simulation here contains the influence of 500 m terrain features, we must assume that the north-to-south variation of the drainage flow out of Eldorado Canyon was caused by, 1) terrain features not resolved by 500 m grid-spacing, 2) multi-scale meteorological interactions (i.e. flow aloft) or 3) inaccuracies in the model formulation. The second cause appears to be most probable because the influence of large-scale terrain features resolved by the 500 m grid-spacing (i.e. the northwest-southeast tributary to Eldorado Canyon) do not appear to have a large influence on drainage direction once it exits the canyon. One would expect that even smaller features have even less influence. One can see in Figure 11, however, that terrain features on the plains which interact with the drainage *after* exiting the main canyon do influence its direction. This is obvious in the case of Ralston Creek Canyon where just beyond the canyon mouth lies the Ralston Butte, which deflects the Ralston drainage to the south.

We conclude from Simulation 2 that, although drainage flows dominated the windflow regime overnight on 4-5 Feb 1991, interactions with upper air flows were quite likely to be present. This multi-scale interaction could explain the north-to-south variation in the observed Eldorado Canyon drainage. Specifically, the possibility exists that interactions with flow aloft imparted southward momentum to the Eldorado flow forcing it to impact the Rocky Flats plant as observed. This effect could not be modeled in the zero initial wind simulations however.

c. Simulation 3: Realistic plains, no mountains

If the Rocky Mountain or canyon drainage flow had little influence on the Rocky Flats tracer dispersion on this night then the drainage generated locally (around Rocky Flats) should be sufficient to reproduce the majority of the plume dispersion features found in Simulation 1. Simulation 3 will also provide information as to how significant, even in stagnant conditions, the Rocky Mountains are to flow structure aloft.

Figure 12 shows the drainage flow that has developed by 0000 5 Feb 1991 in this simulation. This transect crosses through Rocky Flats at approximately 1800 m MSL. Note that significant drainage flows up to 4.0 ms^{-1} have developed. This compares favorably to Simulation 1 which included the Rocky Mountains to the west. This result suggests that sufficient local drainage can develop locally to Rocky Flats to transport pollutants to the east. Other plots of wind vectors and potential temperatures indicate support for this view as well.

A dispersion simulation was also completed to support this conclusion. Compare Figure 13 to Figure 9b, which are from Simulation 3 and Simulation 1, respectively, at 0200-0300 LST 5 Feb 1991. Despite not having the Rocky Mountains to effect its dispersion, Simulation 3 does a similar job to Simulation 1 in both plume width, direction and length. This indicates that although the Rocky Mountains are likely to have some effect on the dispersion of pollutants from Rocky Flats in stable conditions, on 4-5 Feb 1991 locally generated drainage flows, *not Rocky Mountain drainage flows*, were the major influence on dispersion of SF_6.

5. Simulation 4: Realistic topography and winds

After completing our theoretical investigation with zero winds initially we proceeded to compare these simulations to one that included the actual winds for the case night. Unfortunately, no rawinsondes were flown prior to the tracer release in the early evening of 4 Feb 1991. This limited us to initializing the model with a sounding taken at 2000, 4 Feb 1991, within the Rocky Flats compound. Thus we are not able to compare information about the transition period or early evening. Another drawback to initializing with this single sounding (horizontally homogeneous) is that the lowest 100 m of the sounding did not represent the general conditions over the domain based on surrounding observations by tethersondes, towers and surface stations. We chose not to subjectively alter this data and instead allowed the model to prognose changes in the flow. Because the model generally needs a few hours to 'spin-up', comparisons are not likely to be good early in the simulated period, particularly in the lower levels.

a. Simulation 4: Meteorological results

Figure 14 indicates the surface wind vectors at 0100 LST 5 Feb 1991. In comparison to Figure 3, which is the same plot but for the zero-wind initialization, some obvious differences appear. First one notes that the maximum windspeed vector is considerably larger for the real wind simulation (Simulation 4) at 12 ms^{-1} versus 7.8 ms^{-1} for Simulation 1. This difference can be explained by our initialization which had northwesterly winds of 23 ms^{-1} just above the peaks of the Rocky Mountains. Given the high frequency of downslope winds at the surface just to the lee of the peaks, it is likely that some momentum aloft has been transferred to the higher elevations in Figure 14. Secondly, the direction of the vectors just to the east of Rocky Flats are considerably more northerly in the Simulation 4 (Figure 14) versus Simulation 1 (Figure 3). This difference is not as easily explained. It is possible that an interaction with flow aloft has created this change in direction. More surprising than the differences however, are the similarities between the two figures. The model, similar to the case night 4-5 Feb 1991, has formed stable air near the surface while changeable ambient winds are occurring aloft. A comparison of the 0400 LST actual rawinsonde from Rocky Flats with a nearest-gridpoint model extracted sounding (not shown) indicates that the model has done quite well.

The drainage flow that develops in Simulation 4 can be examined by looking at the

u-component winds near the surface (Figure 15). In this case, contours are from 2.0 ms^{-1} to 10 ms^{-1} in 2.0 ms^{-1} increments. This was done to emphasize the drainage flows from the canyons. Canyon influence shows up quite well from north to south, Boulder, Eldorado, Ralston Creek, and Clear Creek Canyons. Missing is a contribution from Coal Creek Canyon, as was measured by Coulter and Martin (1992). Figure 15, however, compares very well to lidar plots of the Eldorado/Coal Creek Canyon drainage onto the plains in Banta (1992), and the evolution of that drainage in time. Banta's(1992) lidar was not able to measure a significant Coal Creek Canyon drainage on the plains, similar to results shown in Figure 15.

b. Simulation 4: Rocky Flats dispersion

The dispersion simulation for Simulation 4 is performed exactly the same as Simulation 1, except for one change; the input meteorological variables. In this dispersion simulation we use the Simulation 4 prognosed fields as input.

The dispersion results from Simulation 4 (Figure 16) can be compared with Figure 9 as an indication of how well the real wind initialization performed. The modeled plume centerline seems (subjectively) to be toward the southeast near the release point whereas Figure 9a indicates a first eastward then northward plume advection. Although the simulated plume for Simulation 4 does contain a westerly component, it appears to have been dominated by the initialized low-level southerly component flow early in the simulation which moves a large concentration of tracer to the north before later advecting it eastward. This difference can, in part, be explained by the Rocky Flats sounding, which indicated predominantly southerly flow in the lower 150 m AGL between 2000 and 2200 LST. However, both plume observations and surrounding measurements indicate winds becoming southwesterly by 2100 LST and westerly by 2200 LST. In this instance, the measurement of southerlies near the surface at Rocky Flats appears to be an outlier from the rest of the data. Consequently, it can be concluded that model initialization under stagnant conditions should include the influence of surrounding stations, either directly or indirectly as an average. Direct inclusion of additional data into the RAMS initialization will be attempted in the near future.

The tendency of the simulated plume to have a northwesterly component near the release point (creating a plume which goes southeast) continues throughout the night as indicated in Figure 16b for the 0200-0300 LST concentration average. The plume width however, appears reasonable compared with observations as does the distance the plume has traveled at each time. Apparently, transport time and diffusiveness are adequately included by the calculated meteorological variables and modified dispersion parameterization above.

7. CONCLUDING REMARKS

In this study, we have focused upon simulating the complex drainage flows that can develop at the mountain-plains interface of the Rocky Mountains. Using the case study day 4-5 February 1991 as an example, it was found that RAMS is capable of simulating realistic drainage flows in complex terrain regions. The results showed that drainage from nearby canyons and the larger-scale Rocky Mountain slope drainage can be a factor in the dispersion of the pollutants released from Rocky Flats. While the primary low-level (<100 m) influence on plume transport around Rocky Flats was the locally developed drainage from the rather gentle slope and terrain variations in the near vicinity of Rocky Flats, the real wind simulations revealed that significant drainage momentum can periodically influence conditions at Rocky Flats. In our simulations, this influence was limited to the large outflow from Eldorado Canyon.

Also, for this case study, multi-scale meteorological interactions were shown to be less significant than drainage near Rocky Flats. This was shown, in part, because the SF_6 dispersion was well depicted by flows produced by a simulation forced exclusively by radiative cooling of the terrain. The coupling of the mesoscale model to an accurate dispersion model appears to be a promising methodology for predicting plume transport. In this case, an actual tracer release was well simulated by our modeling combination. The potential for application of this combination to emergency response problems in other complex terrain regions is obvious.

This experiment also allowed considerable testing to find an optimum model configuration for the mountain-canyon-plains structure of the Rocky Flats region. Gradually increasing the model's resolution from 6 km to 1.5k m to 500 m allowed greater and greater terrain depiction. We found better results when terrain resolution was maximized, in this case at 500 m. Additional experiments at even higher resolution, perhaps 200 m horizontally and 10 m vertically, should be considered to further refine these conclusions.

Acknowledgments. The authors recognize the many ASCOT participants for their contributions to this work. In particular, J.T. Lee and Don Hoard of Los Alamos National Laboratory, are thanked for their commitment of time and helpful suggestions. This research was completed within the ASCOT program as funded by the Department of Energy.

REFERENCES

Chen, C. and W.R. Cotton, 1983a: A one-dimensional simulation of the stratocumulus capped mixed layer. *Bound.-Layer Meteor.*, **25**, 289-321.

Chen, C. and W.R. Cotton, 1983b: Numerical experiments with a one-dimensional higher order turbulence model: Simulation of the Wangara Day 33 case. *Bound.-Layer Meteor.*, **25**, 375-404.

Coulter, R.L. and T.J. Martin, 1991: Argonne National Laboratory Operations During ASCOT 1991. December, Environmental Research Division, Argonne National Laboratory, Argonne, IL 60439.

McNider, R.T., M.D. Moran, and R.A. Pielke, 1988: Influence of diurnal and inertial boundary-layer oscillations on long-range dispersion. *Atmos. Environ.*, **22**, 2445-2462.

Pielke, R.A., 1984: Mesoscale Meteorological Modeling. Academic Press, 612 pp.

Poulos, G.S., and J.E. Bossert, 1992: Large-scale meteorological influences on mountain/valley flows. *CIMA-92 - 22nd International Conference on Alpine Meteorology*, Toulouse, France, September 7-11, 1992, 118-122.

Poulos, G.S., and J.E. Bossert, 1992: A high resolution, complex terrain dispersion study in the Rocky Flats, Colorado Vicinity. *AMS - Tenth Symposium on Turbulence and Diffusion Joint with the Sixth Conference on Mountain Meteorology*, Portland, Oregon, September 29-October 2,1992, J171-J174.

Shearer, D.L., 1991: Summary of Field Test Operations for Rocky Flats TRAC - Winter Validation Study Tests. October, TRC Environmental Consultants.

Tremback, C.J. and R. Kessler, 1985: A surface temperature and moisture parameterization for use in mesoscale numerical models. *Preprints, Seventh Conf. on Numerical Weather Prediction*, Montreal, Amer. Meteor. Soc.

Tremback, C.J., G.J. Tripoli, R. Arritt, W.R. Cotton and R.A. Pielke, 1986 : The regional atmospheric modeling system. *Proc. Inter. Conference on Development and Application of Computer Techniques to Environmental Studies*, November, Los Angeles, California, USA, P. Zannetti, Ed., Computational Mechanics Publications, Boston, 601-607.

Tremback, C.J., and R.L. Walko, 1991: RAMS Version 2c User's Guide (Draft) . Colorado State University, Fort Collins, Colorado, USA, 80523.

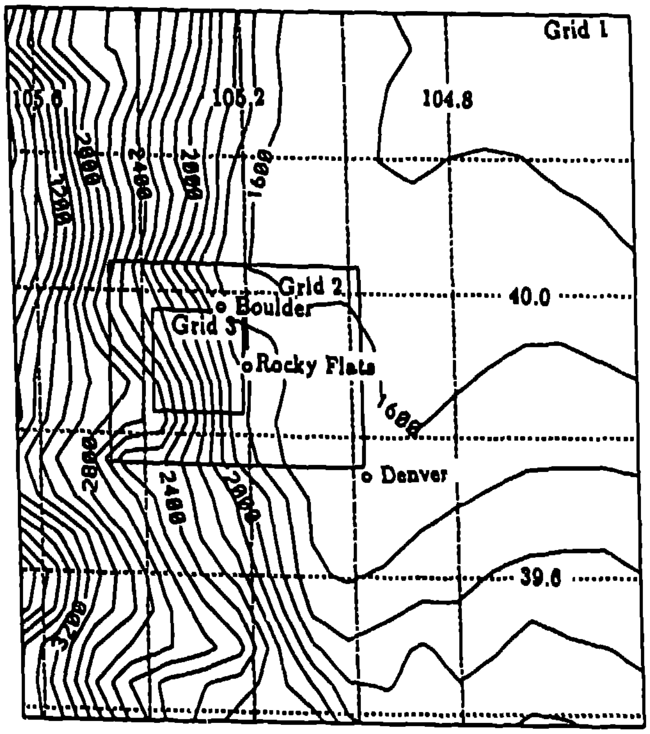

Figure 1. The RAMS model domain used over the Rocky Flats, Colorado region on Grid 1. Contour intervals of terrain and lat-lon lines are 100m and 0.2°, respectively. The two nested grids are also depicted by rectangles to scale.

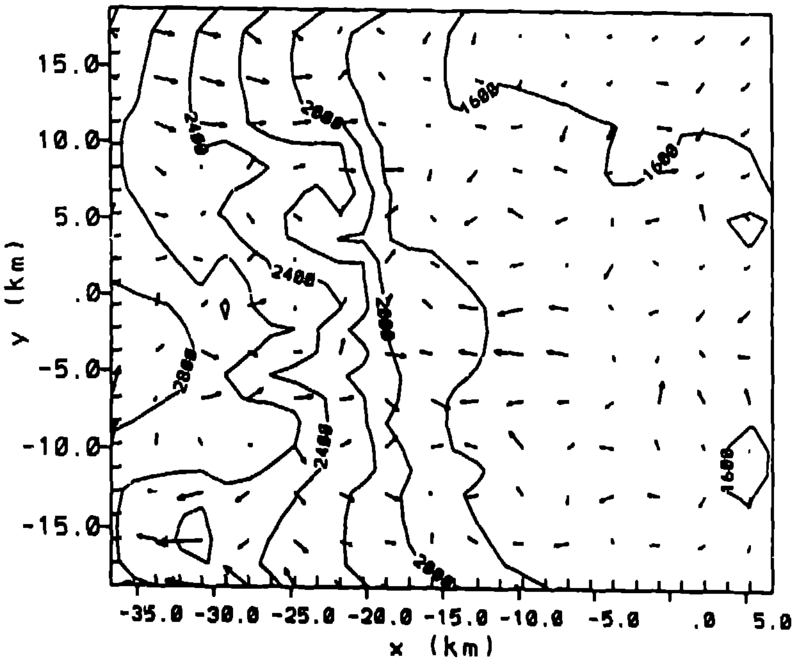

Figure 2. Simulation 1, Grid 2 surface wind vectors at 1730 LST 4 Feb 1991, during the transition from modeled daytime upslope to nighttime drainage winds. The maximum vector is 2.36 ms^{-1}. The interval of terrain contours is 200 m.

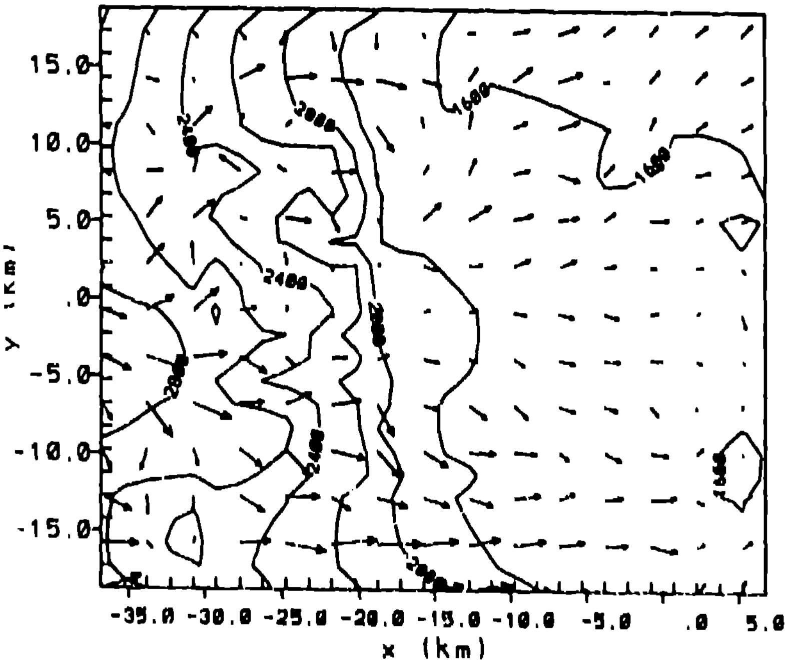

Figure 3. Simulation 1, Grid 2 surface wind vectors at 0400 LST 5 Feb 1991. The maximum vector is 7.89 ms^{-1}. The interval of terrain contours is 200 m.

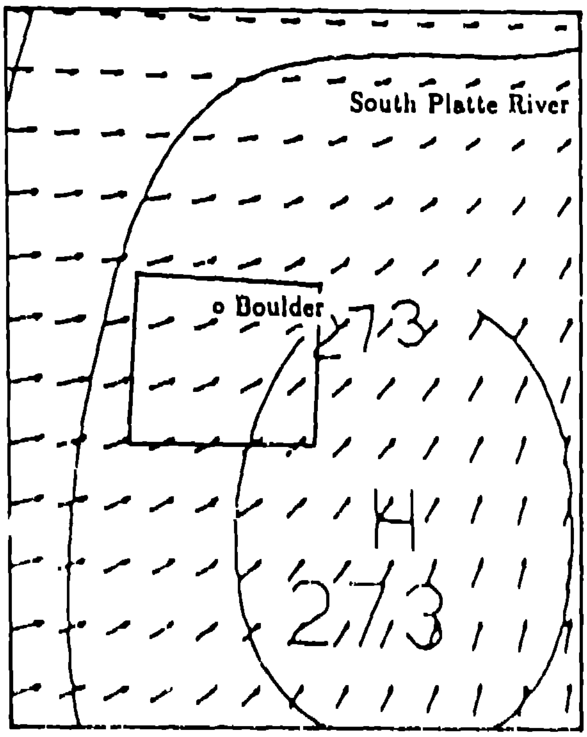

Figure 4. Observed winds for 0400 5 Feb 1991 near Rocky Flats. Grid 2 is depicted by the dashed rectangle for comparison. The maximum vector is 5.3 ms^{-1}.

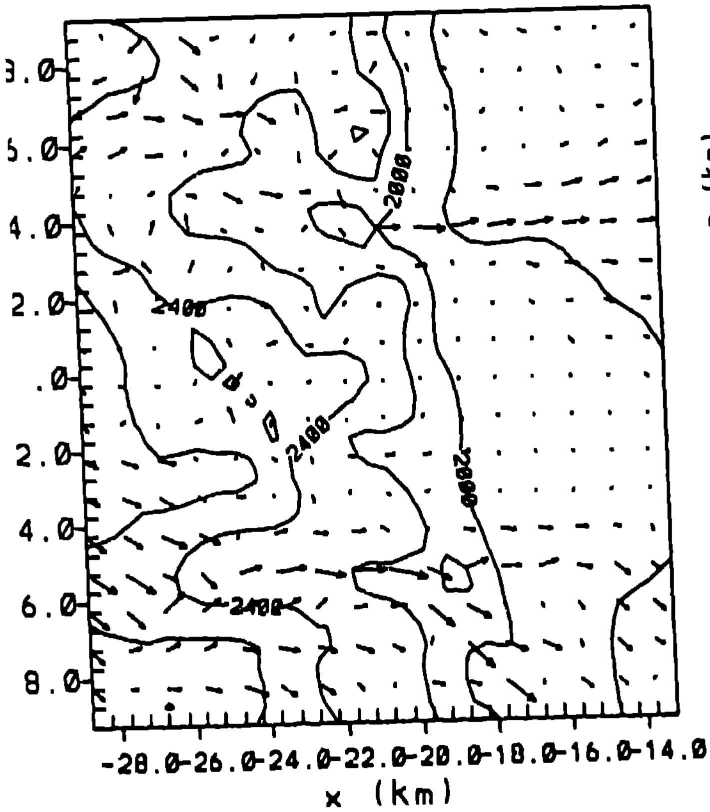

Figure 5. Simulation 1, Grid 3 wind vectors for 50m AGL at 0400 LST, 5 Feb 1991. The maximum vector is 8.96 ms^{-1} and topography contours are every 200m.

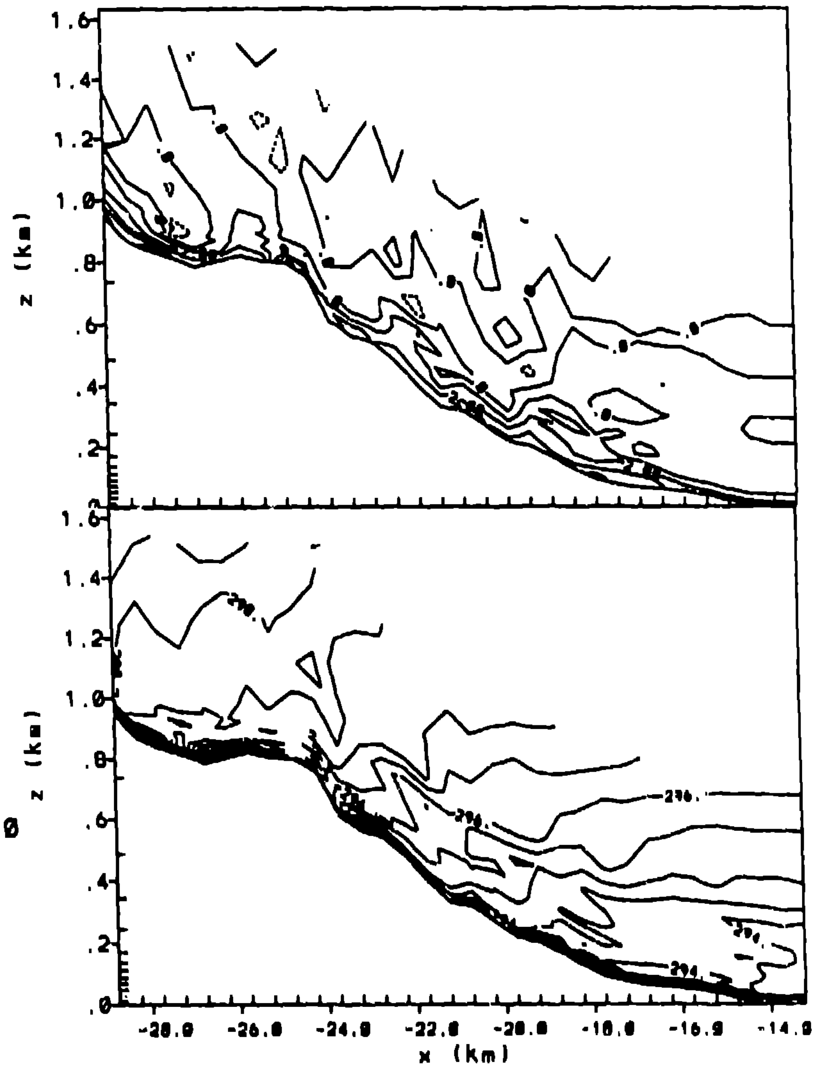

Figure 6. Simulation 1, Grid 3 west-east vertical cross section of (a) U wind component and (b) potential temperature, along the axis of Coal Creek Canyon at 0200 5 Feb 1991. The contour interval is 1.0 ms^{-1} in (a) and 0.5 K in (b).

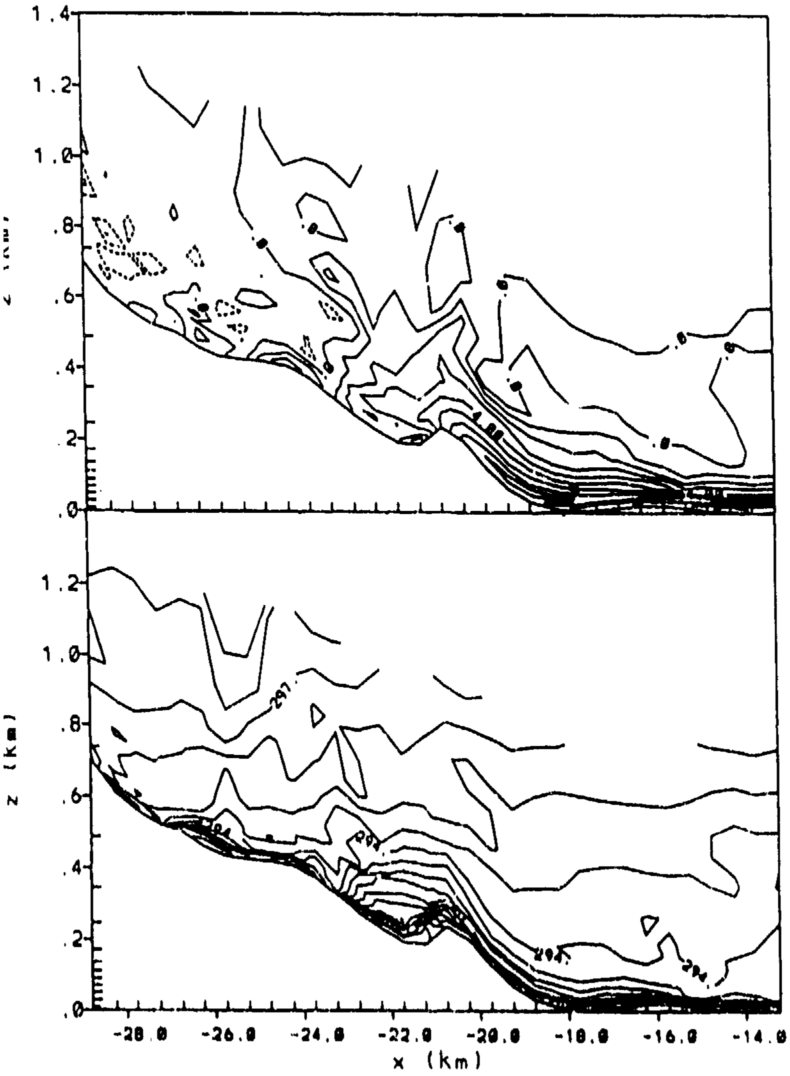

Figure 7. Simulation 1, Grid 3 west-east vertical cross section of (a) U wind component and (b) potential temperature, along the axis of Eldorado Canyon at 0200 5 Feb 1991. The contour interval is 1.0 ms^{-1} in (a) and 0.7 K in (b).

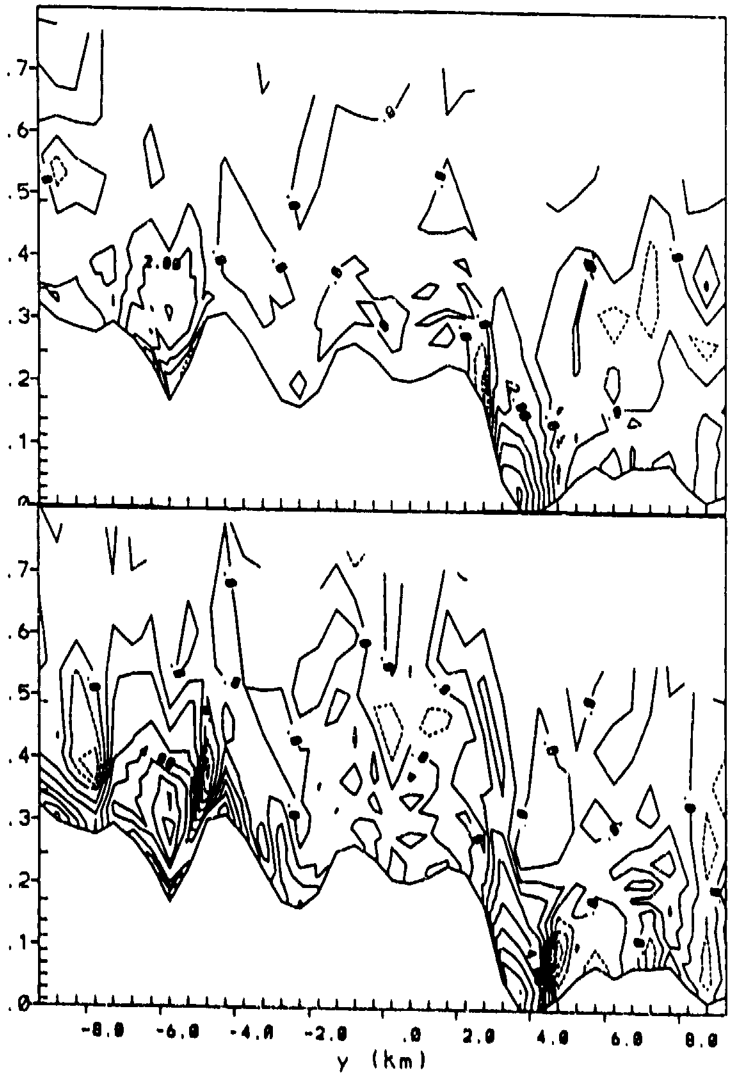

Figure 8. Simulation 1, Grid 3 south-north cross section of U wind component approximately 500m east of the three major canyon's mouths for (a) 2000 and (b) 0200 LST 5 Feb 1991. The contour interval is 1.0 ms^{-1}.

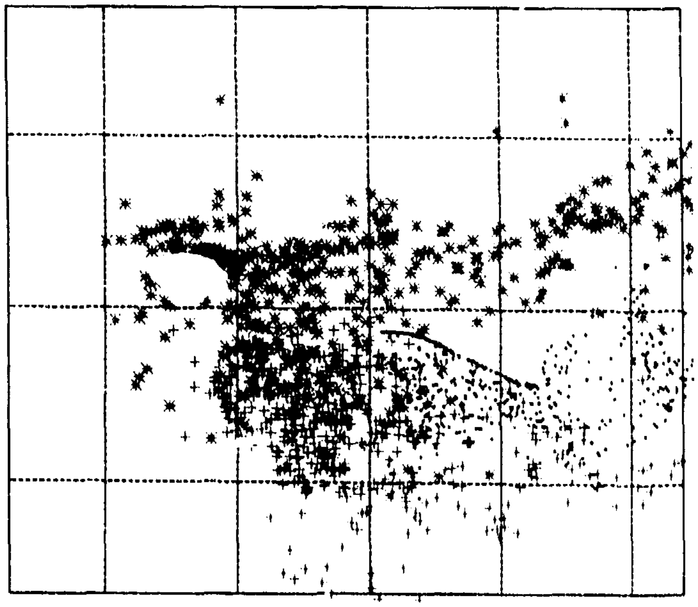

Figure 10. A plan view of particle postions for point sources released within Eldorado and Coal Creek Canyons at 0300 LST 5 Feb 1991. Note that particles released from each canyon tend to take separate transport routes around the Rocky Flats bench.

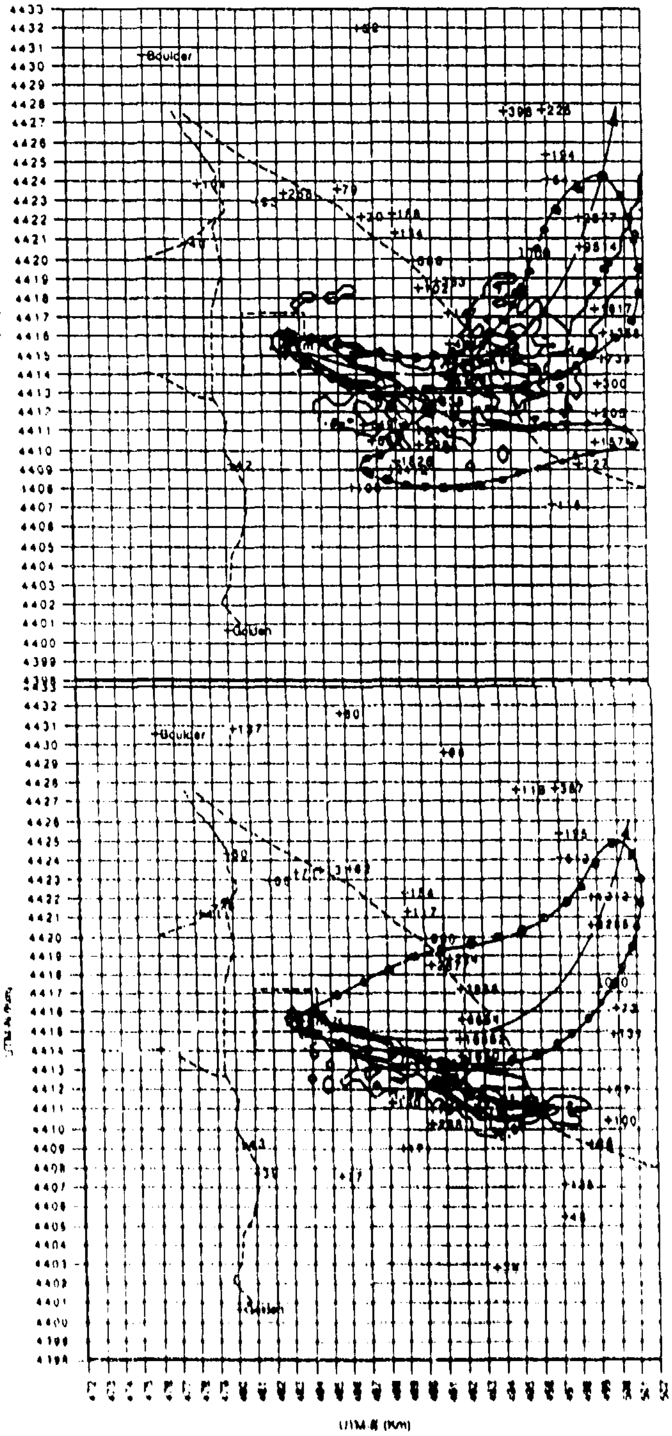

Figure 9. Simulation 1 comparison of simulated (solid contours) versus observed (dotted solid line, 1 μgm^{-3}, from Shearer, 1992) surface SF_6 concentration for averaging periods (a) 2300-0000 and (b) 0200-0300 LST 4-5 Feb 1991. The solid contour intervals from the outermost are 1, 9, 17, 25 and 33 μgm^{-3}, respectively.

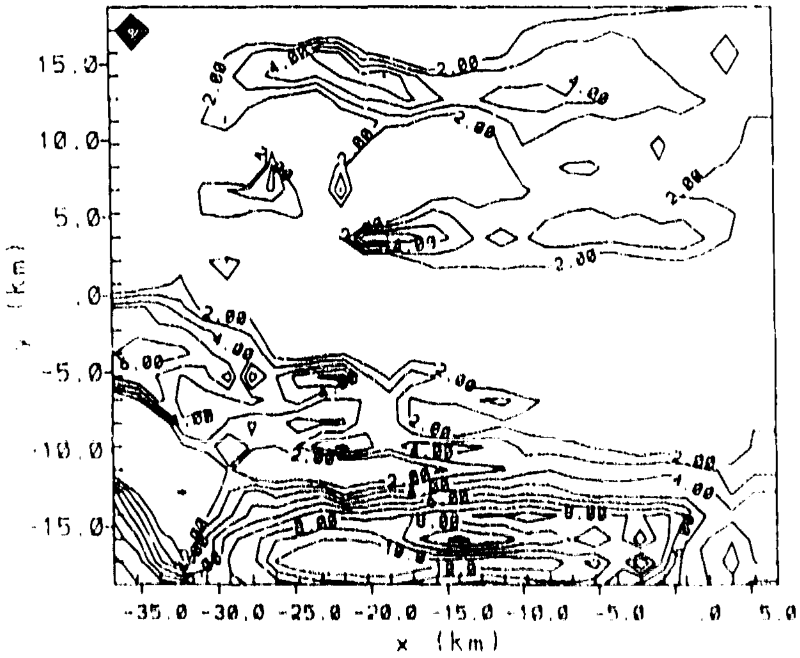

Figure 11. Simulation 2, Grid 2 plan view of U component winds at 50 m AGL for 0400 5 Feb 1991. The contour interval is 1.0 ms^{-1} from a minimum of 2.0 ms^{-1} to a maximum of 10.0 ms^{-1}. Note the drainage flows from the canyons.

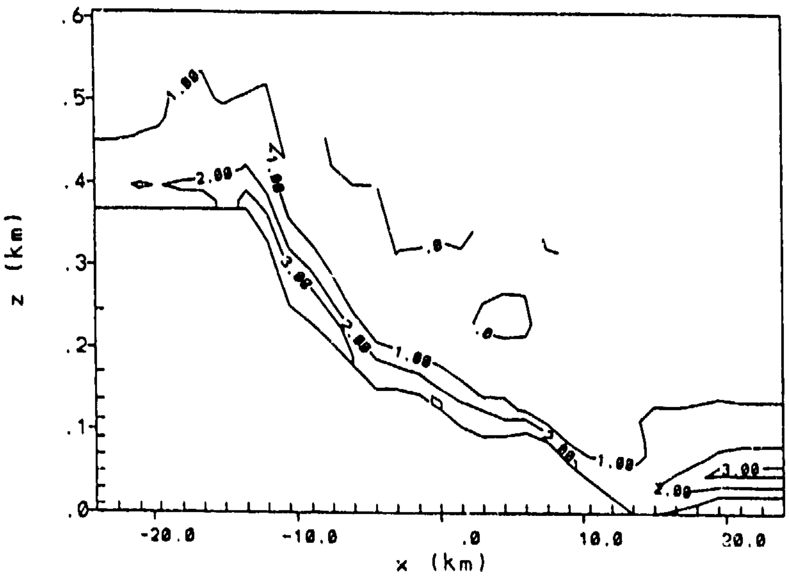

Figure 12. Simulation 3, Grid 1 west-east crossection of U-component winds for 0200 5 Feb 1991. The contour interval is 1.0 ms^{-1}.

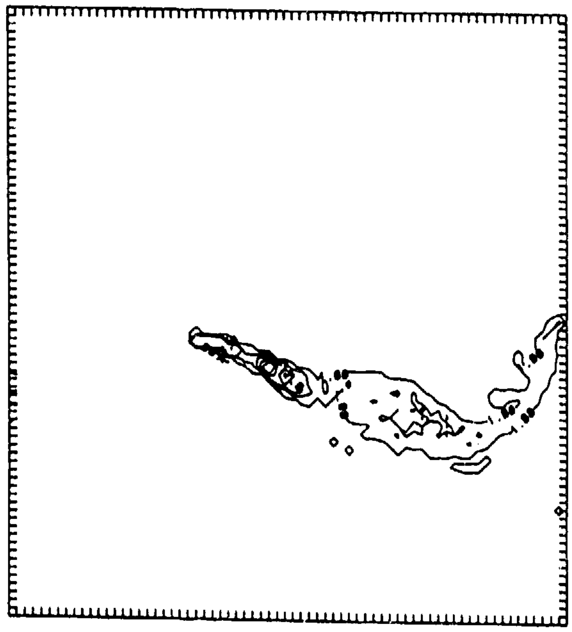

Figure 13. Simulation 3 surface SF_6 concentration for averaging period 0200-0300 LST 5 Feb 1991. The solid contour intervals from the outermost are 1, 9, 17, 25 and 33 μgm^{-3}, respectively.

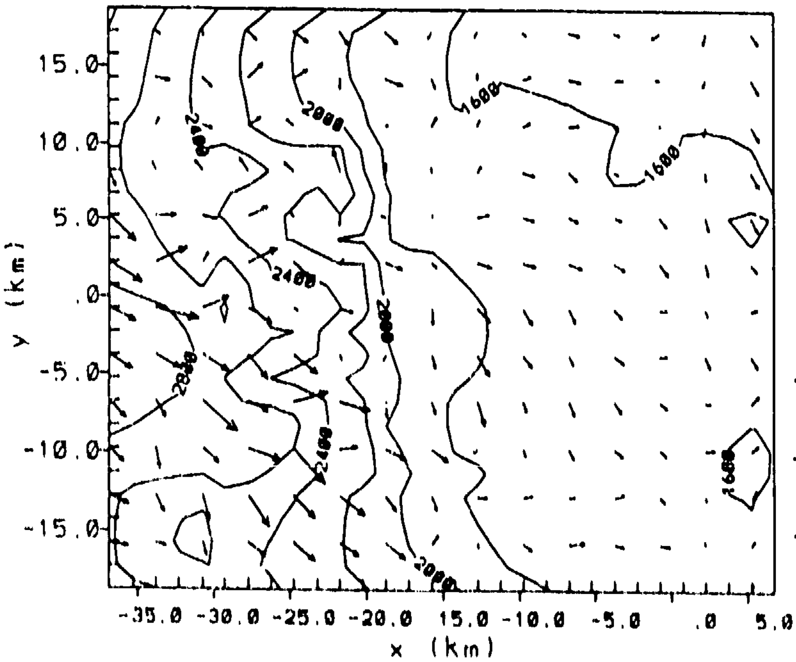

Figure 14. Simulation 4, Grid 2 surface wind vectors at 0400 LST 5 Feb 1991. The maximum vector is 12.06 ms^{-1}. The interval of terrain contours is 200 m.

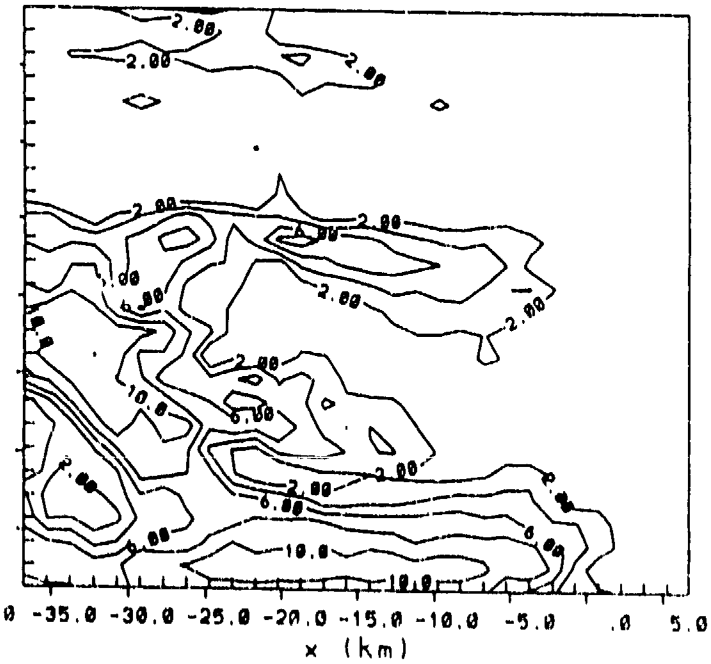

Figure 15. Simulation 4, Grid 2 plan view of U-component winds at 50 m AGL for 0000 5 Feb 1991. The contour interval is 2.0 ms^{-1} from a minimum of 2.0 ms^{-1} to a maximum of 10.0 ms^{-1}. Note the drainage flows from the canyons.

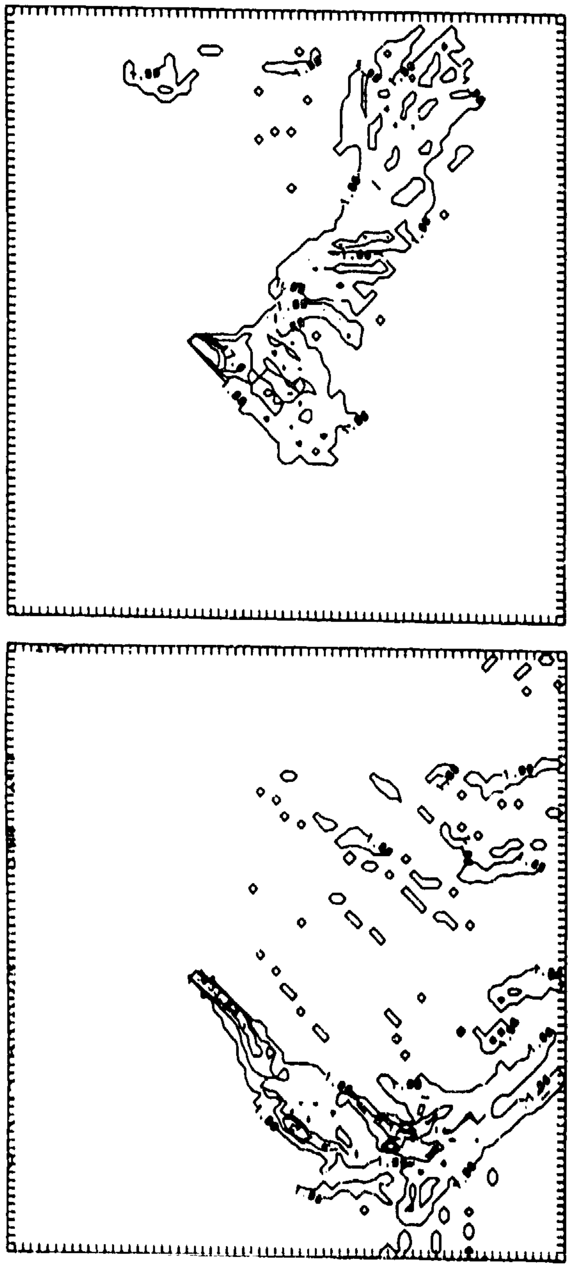

Figure 16. Simulation 4 surface SF_6 concentration for averaging periods (a) 2300-0000 and (b) 0200-0300 LST 4-5 Feb 1991. The contour intervals from the outermost are 1, 9, 17, 25 and 33 $\mu g m^{-3}$, respectively.

END

DATE
FILMED
5/25/93